

## MULTI-OBJECTIVE CONCEPTUAL DESIGN OPTIMIZATION OF A DOMESTIC UNMANNED AIRSHIP

SASAN AMANI, SEID HOSSEIN POURTAKDOUST, FARSHAD PAZOOKI

*Department of Mechanical and Aerospace Engineering, Science and Research Branch, Islamic Azad University,  
Tehran, Iran; e-mail: s.amani@srbiau.ac.ir; pourtak@srbiau.ac.ir; pazooki\_fa@srbiau.ac.ir*

Autonomous airships have gained a high degree of importance over the last decades, both theoretically as well and practically. This is due to their long endurance capability needed for monitoring, observation and communication missions. In this paper, a Multi-Objective Optimization approach (MOO) is followed for conceptual design of an airship taking aerodynamic drag, static stability, performance as well as the production cost that is proportional to the helium mass and the hull surface area, into account. Optimal interaction of the aforementioned disciplinary objectives is desirable and focused through the MOO analysis. Standard airship configurations are categorized into three major components that include the main body (hull), stabilizers (elevators and rudders) and gondola. Naturally, component sizing and positioning play an important role in the overall static stability and performance characteristics of the airship. The most important consequence of MOO analysis is that the resulting design not only meets the mission requirement, but will also be volumetrically optimal while having a desirable static and performance characteristics. The results of this paper are partly validated in the design and construction of a domestic unmanned airship indicating a good potential for the proposed approach.

*Key words:* airship, multi-objective optimization, Pareto optimality

### Nomenclature

|                               |   |  |
|-------------------------------|---|--|
| $x, y, z$                     | – | body fixed coordinates   |
| $X, Y, Z$                     | – | aerodynamic forces   |
| $L, M, N$                     | – | aerodynamic moments  |
| $\alpha, \beta$               | – | angle of attack and side slip angle  |
| $\rho_{air}, \rho_{He}$       | – | air and helium density   |
| $V_0$                         | – | velocity magnitude of point $O$  |
| $\mathbf{F}, \mathbf{T}$      | – | external forces and external moments vector  |
| $\boldsymbol{\omega}$         | – | angular velocity in body coordinates   |
| $m, M'$                       | – | total and added mass   |
| $\mathbf{I}, \mathbf{E}$      | – | moment of inertia tensor and identity matrix   |
| $\mathbf{r}_G$                | – | reference vector from center of gravity to any arbitrary point                               |
| $\mathbf{I}_0, \mathbf{I}'_0$ | – | moment and added moment of inertia about point $O$   |
| $\mathbf{F}_0$                | – | external forces acting through point $O$   |
| $l_{f1}, l_{f2}$              | – | $x$ -distance from origin to the aerodynamic and geometric center of fins                    |
| $l_{f3}$                      | – | $y, z$ -distance from origin to the aerodynamic center of fins                               |
| $l_{gx}, l_{gz}$              | – | $x$ - and $z$ -distance from origin to the aerodynamic center of gondola                     |
| $C_{X_u}$                     | – | derivative of $C_X$ (axial force coefficient) with respect to the translational velocity $u$ |

|               |   |   |
|---------------|---|---|
| $C_{Y\beta}$  | – | derivative of $C_Y$ (lateral force coefficient) with respect to sideslip angle    |
| $C_{Z\alpha}$ | – | derivative of $C_Z$ (normal force coefficient) with respect to angle of attack    |
| $C_{L\beta}$  | – | derivative of $C_L$ (rolling moment coefficient) with respect to sideslip angle   |
| $C_{M\alpha}$ | – | derivative of $C_M$ (pitching moment coefficient) with respect to angle of attack |
| $C_{N\beta}$  | – | derivative of $C_N$ (yawing moment coefficient) with respect to sideslip angle    |
| $a_1, a_2$    | – | parts of the semi-major axis of ellipse   |
| $b$           | – | semi-minor axis of ellipse  |
| $S_f, S_g, A$ | – | fin area, area of gondola and reference area, respectively                        |
| $D, C_D$      | – | drag force exerted and drag coefficient on the airship body                       |

## 1. Introduction

Airships have gained significant attention for municipal and industrial applications since the 1980s. There are a few key reasons contributing to this fact. First, they exploit the natural buoyancy effect for descending and hovering purposes that greatly reduces expenditure of extra energy for these tasks. Second, they are able to operate at low to medium altitudes required for many civilian and surveillance missions such as monitoring, observation and communication link purposes. In addition, these lighter than the air (LTA) vehicles need a lower resolution camera for monitoring purposes, making them superior to Low Altitude Orbit (LEO) satellites for Earth observations. These facts make the airship an ideal candidate for surveillance, reconnaissance and communication relays.

There are generally two approaches available for the design of hybrid airships. The first and more conventional approach is to rely on experienced designers to select the appropriate configuration and components using the available exclusive or proprietary data bases. The second and recently favored approach is through MOO techniques to attain the optimal configuration. The latter approach is followed in this paper, which produces a design that while meeting the mission requirements, optimizes the aerodynamic drag, static stability and performance indices as well as the airship geometry. The latter objective also affects the construction cost of the airship. In other words, the MOO approach allows the designer to select the best configuration which optimizes a series of previously mentioned objectives at the same time. According to the literature, some previous researches considered the aerodynamic discipline in the optimal airship shape design (Lutz and Wagner, 1998; Nejati and Matsuuchi, 2003; Wang and Shan, 2006). The effect of the structure and solar energy in the airship design was also investigated (Wang *et al.*, 2009; An *et al.*, 2007). Wang *et al.* (2009) used Simulated Annealing (SA) to minimize a composite single-objective function consisting of volumetric drag, structural stress, surface area and solar arrays. An *et al.* (2007) considered minimization of drag and structural weight using the MOO approach. They also determined forbidden design regions to be avoided. Wang *et al.* (2011) studied a winged airship design (high altitude stratospheric platform) and focused on verifying merits of lift to buoyancy ratio and its effects on the airship hull sizing and usage of solar energy. A thorough study of the previous works reveals that objectives such as static stability and performance characteristics as well as factors affecting the construction cost has so far not been considered.

In this study, the MOO design approach is considered with new contributions to those previously utilized by researchers, An *et al.* (2007). First, the complete airship configuration including the tail and gondola are taken into account. Second, the static stability as well as performance (related to glide range) characteristics plus the production cost related to the hull surface and volume are considered as objectives. Considering the above objectives, an optimal configuration that simultaneously satisfies a number of objectives is determined using the results of several paretos. Finally, the proposed design configuration is implemented in the real world

to verify the pragmatic aspects of the proposed MOO conceptual design approach.

This paper is arranged as follows: Section 2 deals with the problem formulation and representation of the airship six degree of freedom nonlinear model used to evaluate the gliding distance traveled by the airship. Stability derivatives are discussed in Section 3 as a reference for static stability and performance requirements. Optimal configuration design is the subject of Section 4 where discussions are made about the optimality definition of the airship configuration, the utilized objective functions as well as the design variables. MOO and genetic algorithm are the subjects of Sections 5 and 6, respectively. Section 7 presents simulations followed by discussion of the results. Conclusions are drawn in Section 8 followed by a description of the future work under consideration by the authors.

## 2. Problem formulation

In this section, the governing dynamic equations for the nonlinear airship are presented. The assumptions that lead to these equations as well as the utilized coordinate system are discussed. The interested reader can refer to Mueller *et al.* (2004), for more information about the details of the nonlinear model development. It is important to note that the presented equations will be utilized to calculate the distance traveled by the airship.

### 2.1. Airship model

The airship configuration plus fins and gondola position are depicted in Fig. 1. According to the airship configuration shown in this figure, three fins are mounted in the aft section of the airship. These include two elevators (right and left) for longitudinal control and two rudders (top and bottom) for lateral-directional control purposes.

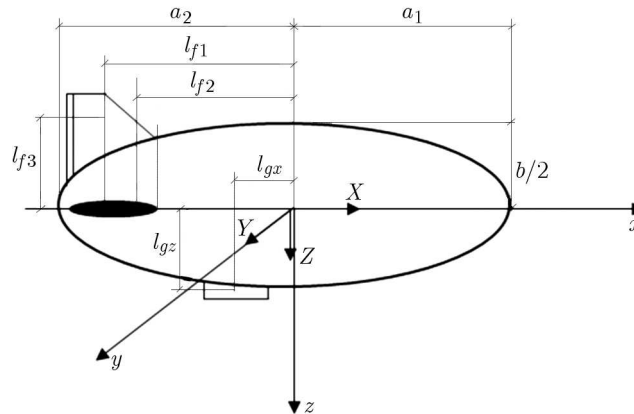


Fig. 1. Airship configuration

### 2.2. Equations of motion

The six degree of freedom dynamic equations for a rigid body in the inertial frame are written in accordance to the basic laws of translational and rotational motion (Mueller *et al.*, 2004)

$$m\dot{\mathbf{v}} = \mathbf{F} \quad \mathbf{I}\dot{\boldsymbol{\omega}} + \boldsymbol{\omega} \times \mathbf{I}\boldsymbol{\omega} = \mathbf{T} \quad (2.1)$$

The moment equations are written about the center of gravity (CG). For flight dynamic analysis, the airship is assumed to be a rigid body. The effects of the added mass and inertia are also taken into consideration. According to the geometry shown in Fig. 2, it is possible to transform

Equations (2.1) from CG to any other arbitrary point within the body. For airships, this point is the so called the center of buoyancy (CB), denoted by  $O$ .

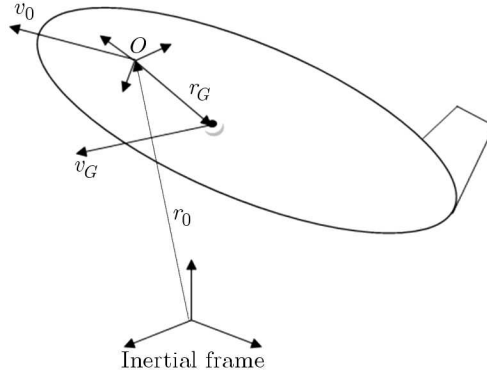


Fig. 2. Coordinate frames

Since the inertial frame has no rotation, it is possible to write the relative velocities by

$$\mathbf{v}_G = \mathbf{v}_O + \mathbf{v}_{G/O} \quad \mathbf{v}_G = \mathbf{v}_O + \boldsymbol{\omega} \times \mathbf{r}_G \quad (2.2)$$

Now it is possible to differentiate Eq. (2.2)<sub>2</sub> and obtain the translational equation of motion in the body axis system

$$m(\dot{\mathbf{v}}_O + \boldsymbol{\omega} \times \mathbf{v}_O - \mathbf{r}_G \times \dot{\boldsymbol{\omega}} + \boldsymbol{\omega} \times (\boldsymbol{\omega} \times \mathbf{r}_G)) = \mathbf{F}_O \quad (2.3)$$

A similar procedure leads to the rotational equation of motion (about point  $O$ ) in the body axis system as well

$$\mathbf{I}_O \dot{\boldsymbol{\omega}} + \boldsymbol{\omega} \times (\mathbf{I}_O \boldsymbol{\omega}) + m \mathbf{r}_G \times (\dot{\mathbf{v}}_O + \boldsymbol{\omega} \times \mathbf{v}_O) = \mathbf{T} \quad (2.4)$$

Combining equations (2.3) and (2.4), the coupled nonlinear equations will become

$$\begin{bmatrix} m\mathbf{E} & -m\mathbf{r}_G^* \\ m\mathbf{r}_G^* & \mathbf{I}_O \end{bmatrix} \begin{bmatrix} \dot{\mathbf{v}}_O \\ \dot{\boldsymbol{\omega}} \end{bmatrix} + \begin{bmatrix} m(\boldsymbol{\omega} \times \dot{\mathbf{v}}_O + \boldsymbol{\omega} \times (\boldsymbol{\omega} \times \mathbf{r}_G)) \\ \boldsymbol{\omega} \times (\mathbf{I}_O \boldsymbol{\omega}) + m\mathbf{r}_G \times (\boldsymbol{\omega} \times \mathbf{v}_O) \end{bmatrix} = \begin{bmatrix} \mathbf{F}_O \\ \mathbf{T} \end{bmatrix} \quad (2.5)$$

where  $\mathbf{r}_G^*$  is the skew symmetric matrix made out of  $\mathbf{r}_G$

$$\mathbf{r}_G^* = \begin{bmatrix} 0 & -z & y \\ z & 0 & -x \\ -y & x & 0 \end{bmatrix} \quad \mathbf{r}_G = \begin{bmatrix} x \\ y \\ z \end{bmatrix} \quad (2.6)$$

Finally, the six degree of freedom nonlinear equations of motion for a rigid body moving through a fluid medium with respect to the CB is given by

$$\begin{bmatrix} m\mathbf{E} + \mathbf{M}' & -m\mathbf{r}_G^* \\ m\mathbf{r}_G^* & \mathbf{I}_O + \mathbf{I}'_O \end{bmatrix} \begin{bmatrix} \dot{\mathbf{v}}_O \\ \dot{\boldsymbol{\omega}} \end{bmatrix} + \begin{bmatrix} m(\boldsymbol{\omega} \times \dot{\mathbf{v}}_O + \boldsymbol{\omega} \times (\boldsymbol{\omega} \times \mathbf{r}_G)) \\ \boldsymbol{\omega} \times (\mathbf{I}_O \boldsymbol{\omega}) + m\mathbf{r}_G \times (\boldsymbol{\omega} \times \mathbf{v}_O) \end{bmatrix} = \begin{bmatrix} \mathbf{F}_O \\ \mathbf{T} \end{bmatrix} \quad (2.7)$$

The aerodynamic and stability derivatives are a function of the airship geometry and flight conditions which are estimated using the Digital Datcom software released for public use (Datcom+Pro version 3.0).

It is important to note that the aforementioned motion equations are used to estimate the airship performance in terms of the distance traveled as one of the key objectives. The traveling distance in a finite time is among the objectives considered, which is directly related to the overall airship configuration sizing.

### 3. Stability derivatives

Stability derivatives play an important and critical role in the determination of static stability and performance characteristics of an airship. They show the sensitivity of aerodynamic force and moment coefficients with respect to flight, atmospheric and control parameters. In turn, the stability and control derivatives are functions of the configuration sizing parameters and the flight condition of the airship. For example, extremely large values of  $C_{X_u}$  will ruin the airship performance in attaining the desired translational velocity and, in return, the requirement of higher range or the distance to be travelled. However, a very small value of this derivative may not satisfy the desired static stability requirements.

Naturally, the above statement necessitates the use of a trade-off study to reach a balanced value of the stability derivatives. This task is handled by the MOO procedure, a subject that will be addressed in Section 4. Table 1 summarizes some of the key longitudinal and lateral-directional stability derivatives for the airship.

**Table 1.** Longitudinal and lateral-directional stability derivatives criteria

|     | $u$            | $v$         | $w$         | $\alpha$             | $\beta$            |
|-----|----------------|-------------|-------------|----------------------|--------------------|
| $X$ | $< 0$          | $\approx 0$ | $\approx 0$ | $\approx 0$          | $\approx 0$        |
|     | $*C_{X_u} < 0$ |             |             |                      |                    |
| $Y$ | $\approx 0$    | $< 0$       | $\approx 0$ | $\approx 0$          | $C'_{Y_\beta} < 0$ |
| $Z$ | $\approx 0$    | $\approx 0$ | $< 0$       | $*C_{Z_\alpha} < 0$  | $\approx 0$        |
| $L$ | $\approx 0$    | $\approx 0$ | $\approx 0$ | $\approx 0$          | $< 0$              |
|     |                |             |             |                      | $C_{L_\beta} < 0$  |
| $M$ | $\approx 0$    | $\approx 0$ | $\approx 0$ | $< 0$                | $\approx 0$        |
|     |                |             |             | $**C_{M_\alpha} < 0$ |                    |
| $N$ | $\approx 0$    | $\approx 0$ | $\approx 0$ | $\approx 0$          | $> 0$              |
|     |                |             |             |                      | $C_{N_\beta} > 0$  |

\* The value of these derivatives should be negative for stability because it is assumed that the aerodynamic coefficients have the same sign as the aerodynamic forces.

\*\* The contribution of airship hull on this derivative is positive because the produced lift will produce a positive pitching moment.

### 4. Optimal configuration design

In this section, the optimality criteria needed for the MOO are addressed. It is assumed that the airship consists of the main hull, tail mounted elevators, rudders and gondola. Clearly, the shape of the hull, the reference area and position of the stabilizers and gondola play an important role in the static stability and performance (distance traveled) of the airship. On the other hand, the configuration sizing and the helium mass determines the major cost of the construction. In order to have a better view of the optimization procedure, Fig. 3 is provided to illustrate the optimization loop and flowchart.

In this paper, the following optimization objectives are considered. The aerodynamic drag coefficient is sought to be minimized. The hull surface area and, in turn, the helium mass are to be minimized in order to reduce the production cost. The glide distance traveled by the airship is to be optimized to meet the customer stipulated requirement. Stability derivatives are to be optimized in order to make the airship resistant to initial disturbances, while keeping an acceptable performance (trade-off).

Mathematically speaking, the above objectives need to be modeled for optimization.

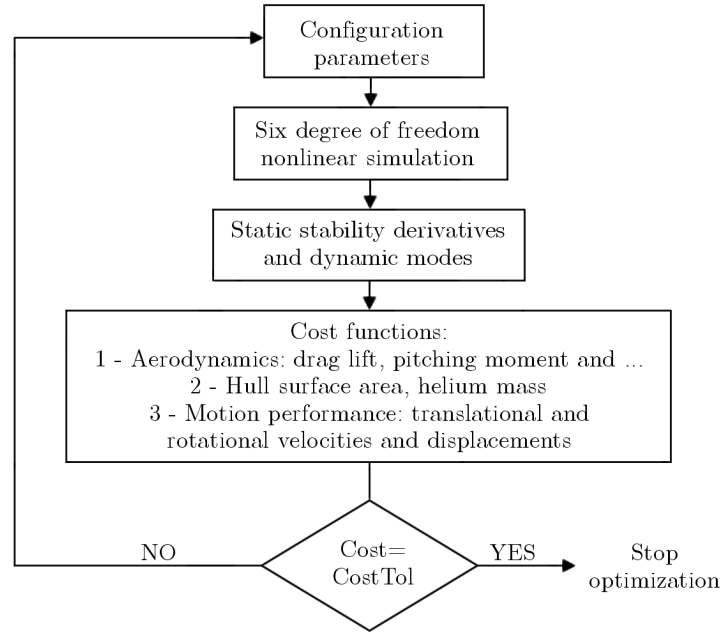


Fig. 3. Optimization flowchart

For the aerodynamic drag, the drag force exerted on the airship is to be minimized (Mueller *et al.*, 2004)

$$D = \frac{1}{2} \rho_{air} V_0^2 A C_D \quad (4.1)$$

For the airship hull surface area, the following objective is to be minimized (web-formulas)

$$S = 2\pi \left( \sqrt[p]{\frac{2a_1^p b^p + b^{2p}}{3}} + \sqrt[p]{\frac{2a_2^p b^p + b^{2p}}{3}} \right) \quad (4.2)$$

where  $p$  is a constant equal to 1.6075. The helium mass is obtained as follows

$$m_h = \frac{2}{3} \rho_{He} \pi (a_1 + a_2) b^2 \quad (4.3)$$

In this equation, the glide distance traveled will be optimized according to the following objective function

$$DT = \sqrt{x_{final}^2 + y_{final}^2 + z_{final}^2} \quad (4.4)$$

where  $DT$  – distance traveled.

**Table 2.** Boundaries of the design variables

| Configuration parameters | Boundaries      | Configuration parameters | Boundaries      |
|--------------------------|-----------------|--------------------------|-----------------|
| $b$                      | $[2.14, 3.57]m$ | $l_{f3}$                 | $[1, 1.74]m$    |
| $a_1$                    | $[5, 7.14]m$    | $l_{gx}$                 | $[1.75, 2.25]m$ |
| $a_2$                    | $[120, 12.85]m$ | $l_{gz}$                 | $[2.28, 3.8]m$  |
| $l_{f1}$                 | $[7, 9]m$       | $S_f$                    | $[9, 27]m$      |
| $l_{f2}$                 | $[7, 78.10]m$   | $S_g$                    | $[0.5, 1.5]m$   |

The key stability derivatives and their desired signs as objectives to be met are tabulated in Table 1. The design variables are those defining the airship geometry which be led to their

optimum set via a genetic algorithm. The design variables are illustrated in Fig. 1, while their boundaries are presented in Table 2.

Considering the previous notations, deriving the airship geometrical parameters in a manner that optimizes our objectives (Eqs. (4.1)-(4.4)) simultaneously, there arises a need for the MOO that is further discussed in the next section.

## 5. Multi-objective optimization

In many optimization problems, there exist several complementing objectives like minimizing the fuel and time. In such cases, it is possible to form an aggregate form of the objectives in one cost function, while allowing for weight coefficients to show the relative importance of each objective. This concept arises the meaning of single-objective optimization. However, in the MOO methodology, objectives are usually conflicting and must be optimized simultaneously without giving special attention to any objective. Consequently, a set of optimal solutions will be generated called the Pareto front. Therefore, instead of one optimal solution (single-objective optimization), a set of optimal solutions can be usually generated (Censor, 1997).

## 6. Genetic algorithm

A genetic algorithm is a global search stochastic optimization strategy that resembles the natural biological behavior and is based on the hypothesis that the nature gives more opportunity of survival to individuals who are more worthy. In other words, the main idea behind the genetic algorithm is to give more opportunities to better results (generations) in order to guide the solution toward its optimal set. The genetic algorithm is an elitist one. Regardless of its structure, this heuristic method is implemented via three operations denoted by reproduction, cross-over and mutation.

Individuals are generated according to their objective values at the reproduction stage. The cross-over is a genetic operator to change the intrinsic value of one chromosome from one generation to another. In other words, the cross-over reproduces the new individuals by combining random information in the mating pool. The mutation operator preserves the diversity of the algorithm in the search space. Because of the fact that in most of the heuristic methods, there is a possibility of getting caught in local minima, several schemes are proposed and used to escape these local minima. A genetic algorithm uses mutation for this purpose (Miller *et al.*, 2010).

## 7. Presentation of results

The simulation results are presented in this section. Subsection 7.1 includes all of the necessary information for the simulation of the previously described airship dynamics. Parameters of the MOO are presented in Subsection 7.2. In Subsection 7.3, drag based optimization that considers drag minimization and the relevant results are presented. Subsection 7.4 considers an analysis to show the effects of static stability derivatives on the performance characteristics of the airship. Subsection 7.5 considers the gliding distance traveled as a requirement for the optimization. Subsection 7.6 presents the results of the proposed optimal design approach for the airship configuration and its real world implementation. Section 8 draws appropriate conclusions and lists possible future related areas of study being considered by the authors.

### 7.1. Airship dynamic parameters

The solver for nonlinear airship dynamic simulation is based on ode3 (Shampine and Reichelt, 1997) with integration time step of one second. The simulation is performed for 100 second, where the initial conditions are given in Table 3.

**Table 3.** Initial conditions of the airship

|          | Initial conditions | Values      |          | Initial conditions | Values  |
|----------|--------------------|-------------|----------|--------------------|---------|
| Body     | $u_0$              | 0.9908 m/s  | Body     | $p_0$              | 0 rad/s |
|          | $v_0$              | -0.0042 m/s |          | $q_0$              | 0 rad/s |
|          | $w_0$              | -0.0042 m/s |          | $r_0$              | 0 rad/s |
| Inertial | $x_0$              | 97.17 m     | Inertial | $\phi_0$           | 0 rad   |
|          | $y_0$              | 0.2075 m    |          | $\theta_0$         | 0 rad   |
|          | $z_0$              | 2500 m      |          | $\psi_0$           | 0 rad   |

### 7.2. Multi-objective optimization parameters

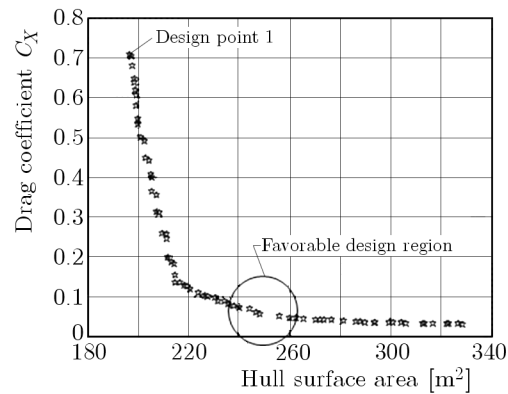
The Multi-Objective Genetic Algorithm (MOGA) parameters are presented in Table 4.

**Table 4.** Multi-objective genetic algorithm (MOGA) parameters

| MOGA parameters       | Values  |
|-----------------------|---|
| Population size       | $15 \cdot \text{number of variables} = 105$   |
| Number of generations | $200 \cdot \text{number of variables} = 1400$ |
| Tournament size       | 2   |
| Cross over fraction   | 0.8   |
| Migration fraction    | 0.2   |

### 7.3. Drag based designs

Undoubtedly, drag reduction is one of the most important objectives pursued in many airship preliminary designs. In this paper, the drag is considered to be an objective function (Eq. (4.1)) and its minimization is sought. According to Fig. 4, minimizing the drag coefficient (and therefore the drag itself!) can lead to a larger hull surface area.

**Fig. 4.** Hull drag coefficient versus hull surface area

Accordingly, though minimization of the aerodynamic drag seems to be a good choice, its implementation requires a higher production cost due to the resulting larger hull surface area. Therefore, the authors have proposed a circular region within the Pareto, in which the design point should be selected for equally weighing the two objectives. Similar regions will also be introduced for the other Pareto's as well, all of which would eventually be utilized to select the final best design point.

#### 7.4. Stability based designs

As discussed in Section 3, static stability derivatives are in competition with the performance indices. This section presents the results of a sensitivity analysis to show this competitive nature. In this regard, the effect of hull configuration, position and size of the stabilizers and gondola on two key stability derivatives  $C_{Z_\alpha}$  and  $C_{Y_\beta}$  are investigated, and the pertaining results are shown in Fig. 5.

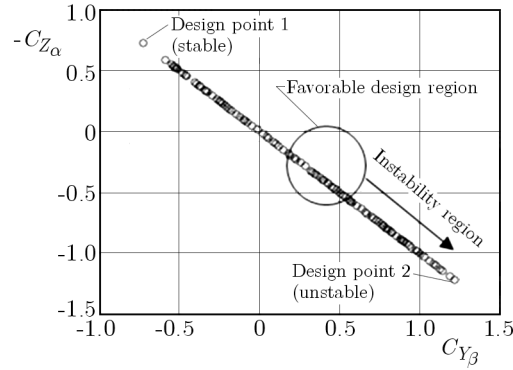


Fig. 5.  $C_{Z_\alpha}$  vs.  $C_{Y_\beta}$  for different configurations

According to Fig. 5, there are several configurations that lead to unstable airship behavior in terms of  $C_{Z_\alpha}$  and  $C_{Y_\beta}$  derivatives. In order to demonstrate their effect, two design points (1 and 2) are chosen to represent the airship dynamics with the initial conditions specified in Table 3. The corresponding six degree of freedom nonlinear airship response is presented in Fig. 6.

Assuming the initial trim condition, Fig. 6 indicates that design point 1 leads to a more stable behavior that is desirable from flying quality point of view. Table 5 is presented to show related configuration sizing parameters for these two points of the Pareto front. According to this table, albeit using point 1 as the design choice brings about several advantages (like more stable behavior, less helium mass and ...), but it has a drawback due to additional expenses required for larger fin areas.

**Table 5.** Comparison of configuration parameters for design points 1 and 2 from Fig. 4

| Airship parameter                   | Design point 1 | Design point 2 |
|-------------------------------------|----------------|----------------|
| Hull length to diameter ratio       | 3.87           | 2.19           |
| Hull surface area [m <sup>2</sup> ] | 203            | 299            |
| Helium mass [kg]                    | 26.53          | 58             |
| Fin area [m <sup>2</sup> ]          | 24             | 10.8           |
| $l_{f1}$ [m]                        | 8.88           | 7.51           |
| $l_{f2}$ [m]                        | 9.80           | 8.29           |
| $l_{f3}$ [m]                        | 1.11           | 1.74           |
| $l_{gx}$ [m]                        | 2.20           | 1.86           |
| $l_{gz}$ [m]                        | 2.43           | 3.80           |

These considerations compact the Pareto to a useful encircled design area shown in Fig. 5. This circular region shows the best design points that satisfy the overall requirements.

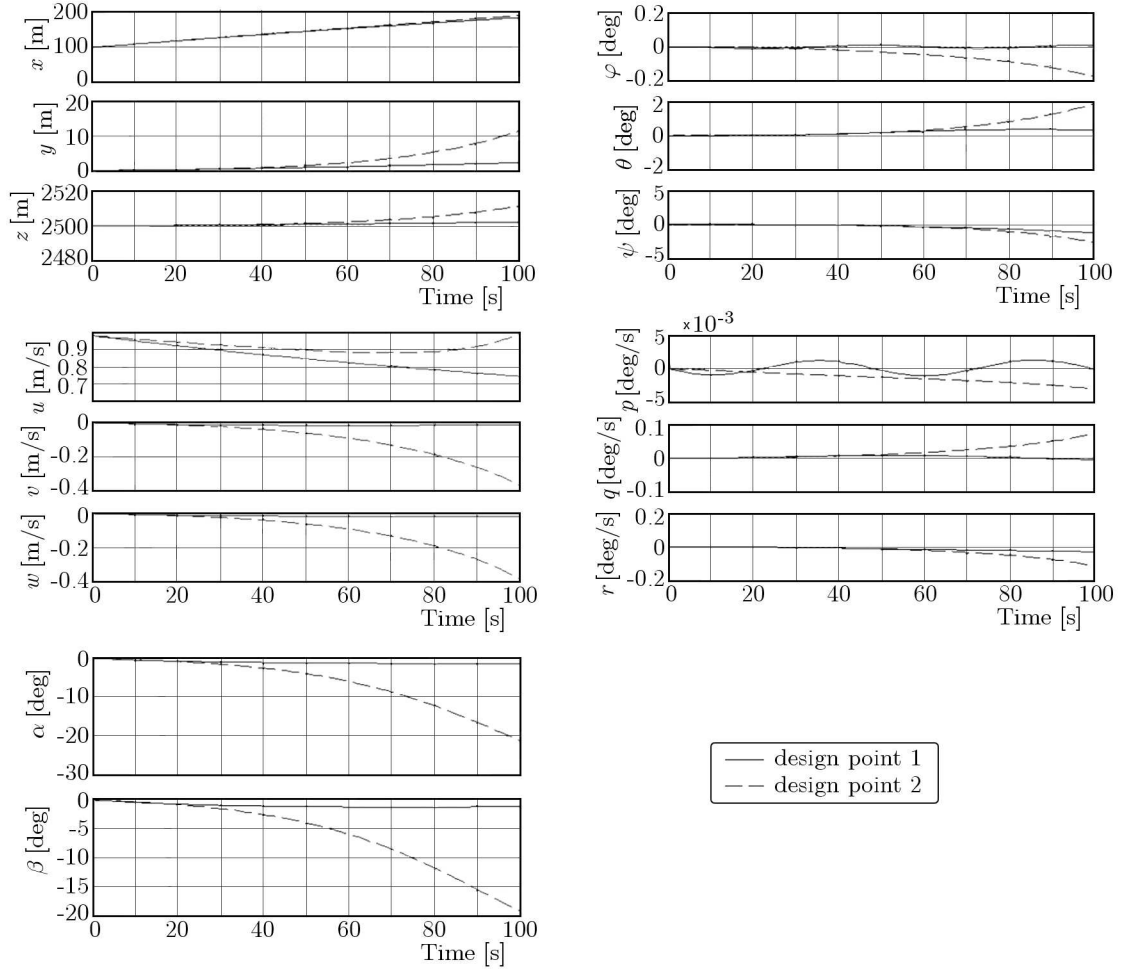


Fig. 6. Six degree of freedom system response for the results shown in Fig. 4

### 7.5. Distance traveled based designs

Figure 7 illustrates the minimum and maximum distances traveled by the airship for various optimized configurations in three dimensional space during 100 seconds of simulation. As shown in this figure, the designer can select an optimum configuration according to glide ranges covered.

For example, design point 1 leads the airship to travel to a totally different location as compared to design point 2. Therefore, the designer can select design point 1 to travel farther. Table 6 presents the difference in configuration sizing parameters of the two design points for the Pareto front shown in Fig. 6.

**Table 6.** Comparison of configuration parameters for design points 1 and 2 from Fig. 7

| Airship parameter                   | Design point 1 | Design point 2 |
|-------------------------------------|----------------|----------------|
| Hull length to diameter ratio       | 3.97           | 3.54           |
| Hull surface area [m <sup>2</sup> ] | 186.6          | 166.81         |
| Helium mass [kg]                    | 23.09          | 20.45          |
| Fin area [m <sup>2</sup> ]          | 24             | 21.36          |
| $l_{f1}$ [m]                        | 8.49           | 7.20           |
| $l_{f2}$ [m]                        | 9.38           | 7.94           |
| $l_{f3}$ [m]                        | 1.05           | 1.04           |
| $l_{gx}$ [m]                        | 2.11           | 1.78           |
| $l_{gz}$ [m]                        | 2.30           | 2.29           |

A notable consequence of the presented table and its related Fig. 6 is that for the airship to glide farther, a larger helium mass is required. This is due to the fact that according to Newton's second law of motion, increasing the mass will decrease the negative acceleration produced by the drag force and which, in turn, causes the airship to move farther in the inertial space.

Again given the above mentioned facts, one can choose a spherical optimum design region shown in Fig. 7. This region satisfies various objectives (like acceptable helium mass) while meeting the required gliding range covered in the inertial space.

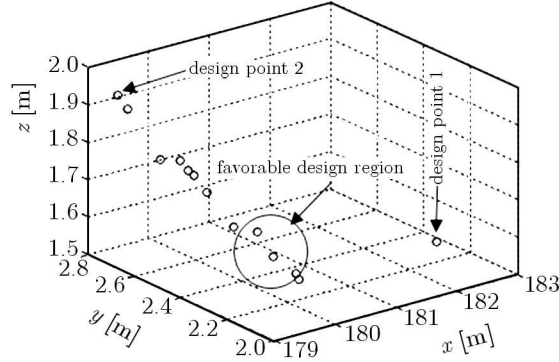


Fig. 7. Final gliding position of the airship in inertial coordinates

A similar approach is taken to show the rotational movement of the airship in terms of the terminal Euler angles. Pertaining results are depicted in Fig. 8. Table 7 demonstrates the configuration parameters corresponding to the design points 1 and 2 from Fig. 8.

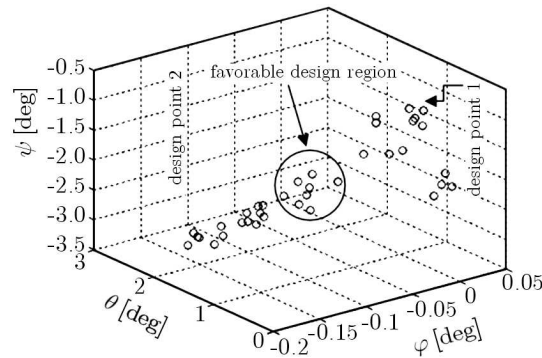


Fig. 8. Final attitude orientation for various configurations

**Table 7.** Comparison of configuration parameters for design points 1 and 2 from Fig. 8

| Airship parameter                   | Design point 1 | Design point 2 |
|-------------------------------------|----------------|----------------|
| Hull length to diameter ratio       | 3.86           | 2.17           |
| Hull surface area [m <sup>2</sup> ] | 260.53         | 285.92         |
| Helium mass [kg]                    | 38.58          | 54.71          |
| Fin area [m <sup>2</sup> ]          | 10.73          | 15.18          |
| $l_{f1}$ [m]                        | 9.03           | 7.18           |
| $l_{f2}$ [m]                        | 9.96           | 7.23           |
| $l_{f3}$ [m]                        | 1.25           | 1.71           |
| $l_{gx}$ [m]                        | 2.24           | 1.78           |
| $l_{gz}$ [m]                        | 2.75           | 3.74           |

Similar to the previous analysis, a spherical optimal design area can be considered that satisfies the needs for reasonable rotational airship maneuver while observing other objectives such as the hull surface area and the helium mass.

Taking all of the above into account, an airship configuration is proposed that lies within the realms of the spherical as well as circular design regions depicted in the Pareto plots. This configuration will be optimal form all aspects considered, namely aerodynamic drag, stability requirement (derivative value or sign), helium mass and hull surface area (production cost) and the gliding distance traveled . It means that the designer can be assured of the selected configuration to show the overall reasonable behavior. The proposed configuration is shown in Fig. 9, next to the configuration which is not Pareto optimal.

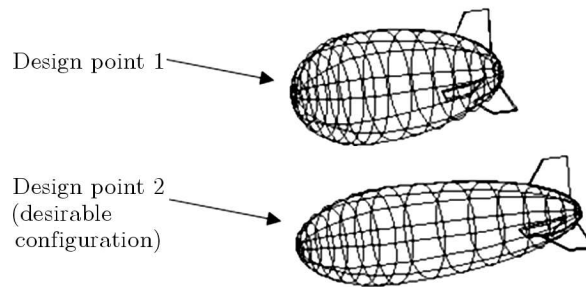


Fig. 9. Two configurations. Design point 1 (not optimal), design point 2 (optimal)

## 7.6. Implementation of the described design procedure

Figure 10 shows a schematic of the constructed airship called NAMA. This airship was built for practical research on LTA buoyancy at 2500 meter altitude and was to withstand wind speeds of up to 13 meters per second.

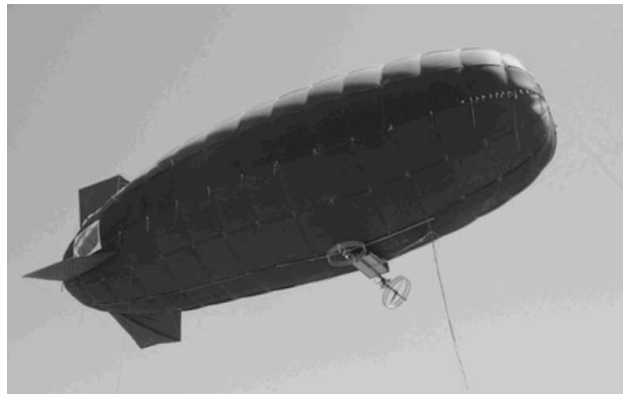


Fig. 10. NAMA, first prototype of the constructed domestic airship

The system is a non-rigid dirigible whose body shape is achieved through preserving a differential pressure (0.05 to 0.2 atmospheres) with the ship outside environment. Obviously, this pressure differential is a function of system endurance, flight duration, ambient temperature and flight altitude. In addition, in order to withstand the high pressure on the vehicle body and skin, advanced materials (Vectran) were used with an ultimate stress capability of up to 3 gigapascal. Vectran is extremely durable and tolerant in harsh environmental conditions such as UV and, at the same time, is lightweight (about 80 gram per meter squared) which makes it a quite appropriate for the airship body skin.

Composite materials forming the inside layer of the body are produced out of thermo plastic polyurethane (TPU) which also has a good tolerance to UV and, additionally, exhibits low permeability against helium leakage. To overcome internal pressure on the body and stitch locations, and also in order to have clamping positions for payload hanging, several circumferential belts were utilized. These belts are spaced out 1 meter apart through the entire length of the body, and each weighs around 1800 kilograms.

## 8. Concluding remarks

Multi objective optimization for the configuration design of a domestic airship is performed considering static stability and flight performance merits. The role of other objectives such as the aerodynamic drag, the airship hull surface as well as the helium mass is also investigated. The latter two objectives directly affect the production cost of the airship. The proposed scheme can produce configurations with different levels of stability. Application of MOO enables the designer to select more efficient designs through consideration of multiple criteria without the need for additional trade off studies. Implementation of the proposed method has been utilized for the design and construction of a prototype domestic airship.

Despite the fact that the presented paper has covered a large and useful class of objective functions for design optimization, other criteria such as the aerodynamic lift and the airship material could also be considered as complementary objectives. In addition, implementation of active controls through vectored thrusters and their optimal placement for station keeping and trajectory management are of high importance. The above issues as well as the flight test results of the first prototype are being utilized by the authors for the future work, results of which will help the improved second prototyping.

## References

1. AN W., LI W., WANG H., 2007. Multi objective optimization design of envelop shape of a certain airship with deviation considered, *Journal of Northwestern Polytechnical University*, **25**, 1, 56-60
2. CENSOR Y., 1977, Pareto optimality in multiobjective problems, *Applied Mathematics and Optimization*, **4**, 41-59
3. Datcom+Pro version 3.0, <http://www.holy cows.net/datcom/>
4. LUTZ T., WAGNER S., 1998, Drag reduction and shape optimization of airship bodies, *Journal of Aircraft*, **35**, 3, 345-351
5. MILLER F.P., VANDAME A.F., MCBREWSTER J., 2010, *Genetic Algorithm*, VDM Verlag Dr. Mueller E.K., ISBN: 6130211791, 9786130211790
6. MUELLER J.B., PALUSZEK M.A., ZHAO Y., 2004, Development of an aerodynamic model and control law design for a high altitude airship, *AIAA 3rd "Unmanned Unlimited" Technical Conference, Workshop and Exhibit 20-23 September 2004*, Chicago, Illinois
7. NEJATI V., MATSUUCHI K., 2003, Aerodynamic design and genetic algorithms for optimization of airship bodies, *JSME International Journal, Series B: Fluids and Thermal Engineering*, **46**, 4, 610-617, doi:10.1299/jsmeb.46.610
8. SHAMPINE L.F., REICHEL T. M.W., 1997. The MATLAB ODE Suite, *SIAM Journal on Scientific Computing*, **18**, 1, 1-22
9. WANG H., SONG B., ZHONG X., 2011, Configuration design and sizing optimization of a winged airship, *International Conference on Network Computing and Information Security*, **2**, 41-45

10. WANG Q.-B., CHEN J.-A., FU G.-Y., DUAN D.-P., 2009. An approach for shape optimization of stratosphere airships based on multi disciplinary design optimization, *Journal of Zhejiang University, Science A*, **10**, 11, 1609-1616
11. WANG X.L., SHAN X.X., 2006, Shape optimization of stratosphere airship, *Journal of Aircraft*, **43**, 1, 283-287
12. [www.web-formulas.com/Math-Formulas/Geometry\\_Surface\\_of\\_Ellipsoid.aspx](http://www.web-formulas.com/Math-Formulas/Geometry_Surface_of_Ellipsoid.aspx)

*Manuscript received February 4, 2013; accepted for print May 17, 2013*